Published in final edited form as:
Arthritis Rheum. 2011 November ; 63(11): 3274–3283. doi:10.1002/art.30573.

CXCL10 and its receptor CXCR3 regulate synovial fibroblast invasion in rheumatoid arthritis

Teresina Laragione[1], **Max Brenner**[1], **Barbara Sherry**[2], and **Pércio S. Gulko**[1,3]

[1]Laboratory of Experimental Rheumatology, Center for Genomics and Human Genetics, Feinstein Institute for Medical Research, Manhasset, NY, 11030

[2]Center for Immunology and Inflammation, Feinstein Institute for Medical Research, Manhasset, NY, 11030

Abstract

Objectives—CXCL10 is expressed in increased levels in highly invasive fibroblast-like synoviocytes (FLS) from arthritic DA rats and rheumatoid arthritis (RA). In this study we analyzed the role of CXCL10 and its receptor CXCR3 on the regulation of the invasive properties of FLS.

Methods—FLS were isolated from synovial tissues of RA patients, and from DA and arthritis-protected Cia5d rats with pristane-induced arthritis. We used an *in vitro* model of invasion through Matrigel, which has been shown to correlate with articular damage in RA and in rat arthritis. FLS were cultured in the presence or absence of CXCL10, anti-CXCR3 antibody, CXCR3 inhibitor AMG487, or controls, then studied for invasion, MMP-1-3 production, intracellular calcium influx and cell morphology.

Results—DA FLS produced higher levels of CXCL10 compared with minimally-invasive Cia5d. CXCL10 treatment increased Cia5d FLS invasion by 2-fold, and this increase was blocked by anti-CXCR3. Both anti-CXCR3 and AMG487 reduced DA FLS invasion by as much as 77%. AMG487 significantly reduced RA FLS invasion 60%. CXCR3 blockade reduced levels of MMP-1 by 58%, inhibited receptor signaling (64%-100% reduction in intracellular calcium influx) and interfered with actin cytoskeleton reorganization and lamellipodia formation in rat and RA FLS.

Conclusion—We describe and characterize a new autocrine/paracrine role for CXCL10-CXCR3 in the regulation of rat and RA FLS invasion. These observations suggest that the CXCL10-CXCR3 axis is a potential new target for therapies aimed at reducing FLS invasion and its associated joint damage and pannus invasion and destruction in RA.

INTRODUCTION

Rheumatoid arthritis (RA) is a chronic autoimmune disease that is associated with increased risk for joint deformities, disability, and reduced life expectancy (1–3). The RA synovial tissue is typically characterized by synovial hyperplasia, also called pannus, which is infiltrated with inflammatory cells. The RA synovial pannus produces pro-inflammatory cytokines, chemokines and proteases, and invades and destroys cartilage and bone (4, 5).

[3]Address correspondence and reprint requests to: Pércio S. Gulko M.D., Laboratory of Experimental Rheumatology, Center for Genomics and Human Genetics, Feinstein Institute for Medical Research, 350 Community Drive, Room 139, Manhasset, NY 11030., Phone: (516) 562-1275, FAX: (516) 562-1153, pgulko@nshs.edu.

The authors have no financial or commercial conflict of interests to disclose.

The fibroblast-like synoviocyte (FLS) has a central role in the formation of the RA synovial pannus and in joint destruction (4, 6).

The *in vitro* invasive properties of FLS derived from patients with RA and from rats with pristane-induced arthritis (PIA) through collagen-rich (Matrigel) have been shown to correlate with radiographic erosive changes and with histological joint damage (7, 8). Erosive changes and joint damage correlate with increased risk for worse disease outcome and reduced functional capacity, including the development of deformities (9–12). Therefore, understanding the regulation of FLS invasion has the potential to generate new targets for therapies aimed at reducing articular damage as well as improving disease outcome.

We have previously studied highly invasive FLS derived from PIA-susceptible DA rats, and compared them with minimally invasive FLS obtained from PIA-resistant strain DA.F344(Cia5d) (7). Microarray analysis of gene expression comparing FLS from these two strains identified a novel invasion-associated gene expression signature (13). This FLS invasion signature included the increased expression of genes implicated in cancer cell invasion as well as other cancer-associated phenotypes (13). CXCL10 (IP-10) was one of the genes with the most significantly increased expression in DA FLS with a 4.6-fold increased expression, compared with DA.F344(Cia5d) congenics (13). CXCL10 is known to be up-regulated in several cancers and to mediate cancer invasion, and its levels correlate with worse prognosis (14–18). Synovial fluid and synovial tissue levels of CXCL10 are also increased in RA patients (19–21), and serum levels of CXCL10 correlate with disease activity (22).

CXCR3 is a seven trans-membrane G protein-coupled receptor for CXCL9, CXCL10 and CXCL11 (23). CXCR3 is expressed by endothelial cells, mast cells, T cells and FLS (23, 24). Therefore, we considered that, in addition to its known chemotactic properties, the increased concentrations of CXCL10 produced by arthritic FLS could mediate cell invasion in an autocrine and paracrine manner via CXCR3, similarly to what is seen in cancer. In this study, we determined that CXCL10 increases the invasive properties of FLS, and that CXCR3 blockade reduces invasion of FLS obtained from arthritic DA rats, as well as FLS from RA patients.

METHODS

Rats

Inbred DA (DA/BklArbNsi, arthritis-susceptible) rats were originally purchased from Bentin-Kingman (Freemont, CA), bred at the Arthritis Branch at the National Institutes of Health (NIH) and then transferred to the the Feinstein Institute (formerly North Shore-LIJ Institute). DA.F344(Cia5d) congenic rats were generated as previously described (25, 26). Briefly, the Cia5d chromosomal interval was introgressed from arthritis-resistant F344 into arthritis-susceptible DA genetic background using a genotype-guided strategy for ten backcrosses. Rats heterozygotes only at the Cia5d interval were then intercrossed to generate homozygote congenics. All animals were housed in a specific pathogen-free environment, with 12-hour light and dark cycles and free access to food and water. All experiments involving animals were reviewed and approved by the Feinstein Institute for Medical Research Institutional Animal Care and Use Committee (IACUC).

Induction of Pristane-induced arthritis (PIA) and tissue collection

Eight to 12 week- old rats received 150 μl of pristane by intradermal injection divided into two sites at the base of the tail (27, 28). On day 21 post-pristane injection, animals were euthanized and synovial tissues collected from the ankle joints for FLS isolation.

RA patients and synovial tissues

Human synovial tissues were obtained from RA patients undergoing orthopedic surgery. All patients met the American College of Rheumatology criteria for RA (29). Informed consent was obtained from all participating subjects under an Institutional Review Board-approved protocol.

Isolation and culture of FLS

FLS were obtained as previously described (7). Briefly, tissues were minced and incubated with a solution containing DNase (0.15mg/ml), hyaluronidase type I-S (0.15 mg/ml), and collagenase type IA (1 mg/ml) (Sigma, St.Louis, MO) in DMEM (Invitrogen, Carlsbad, CA) for 1 hour at 37°C. Cells were washed and re-suspended in complete media containing DMEM supplemented with 10% FBS (Invitrogen), glutamine (300 ng/ml), amphotericin B (250 μg/ml) (Sigma), and gentamicin (20 ng/ml) (Invitrogen). After overnight culture, non-adherent cells were removed and adherent cells cultured. All experiments were performed with FLS after passage four (>95% FLS purity).

AMG487

AMG487 (a gift from Amgen, Thousand Oaks, CA) is a small molecule antagonist of CXCR3 that has a reported CXCL10 IC50 of 0.008 μM (30). It has been shown to effectively block CXCR3 activity in cells from different species, including human and rat.

Invasion Assay

The *in vitro* invasiveness of FLS was assayed in a transwell system using Matrigel-coated inserts from BD (Franklin Lakes, NJ) or Chemicon (Temecula, CA), based on availability, as previously described (7, 8). Briefly, 70–80% confluent cells were harvested by trypsin-EDTA digestion, and re-suspended at 2.0×10^4 cells in 500 μl of serum-free DMEM. Cells were placed in the upper compartment of the Matrigel-coated inserts. The lower compartment was filled with complete media (as described above) and the plates were incubated at 37°C for 24 hours. The upper surface of the insert was then wiped with cotton-swabs to remove non-invading cells and the Matrigel layer. For the BD inserts, the opposite side of the insert was stained with Crystal Violet (Sigma) and the total number of cells that invaded through Matrigel counted at 100X magnification. For the Chemicon inserts, the bottom surface of the insert, which contained the cells that invaded through Matrigel, was stained with the kit staining solution, re-solubilized with acetic acid 10% and the solution absorbance read at 570 nm as directed by the manufacturer's protocol. Experiments with BD inserts were done in duplicate and those with Chemicon inserts in triplicate. Where indicated, mouse recombinant CXCL10 (1 μg/ml) was added to complete medium in the bottom chamber, while mouse anti-human CXCR3 blocking antibody (200μg/ml) or an IgG1 isotype control (200μg/ml) (R&D systems, Minneapolis, MN) or the CXCR3 small molecule antagonist AMG487 (5μM, 10μM or 100μM) (or the diluent DMSO as control) was added to the upper chamber for overnight incubation.

Zymography

FLS were cultured for 24h in the upper chambers of Matrigel-coated inserts. Supernatants were collected from each upper chamber after 24h, then concentrated ten-times with Microcon columns YM-30 (Millipore, Bedford, MA). Same amounts of concentrated protein were mixed with Tris-glycine-SDS sample buffer (Invitrogen), and the mixture loaded into a zymogram pre-casted gel (Invitrogen), and electrophoresed, as previously described (7, 31, 32). After the electrophoresis, gels were treated with renaturing buffer (Invitrogen), followed by overnight incubation in a developing buffer (Invitrogen) at 37°C. Gels were stained with SimplyBlue Safe-Stain (Invitrogen) for 1 hour at room temperature, and then

washed extensively. Gelatin zymography was used to assess MMP-2, and casein zymography was used for MMP-3 (7, 33)

Western blot analysis

MMP-1 detection in FLS culture supernatants—Equal volumes of the upper chambers' supernatants (as described in the zymography section) were loaded into a NuPAGE 10% Bis-Tris gel (Invitrogen) in the presence of MES buffer (Invitrogen) and electrophoresed under reducing conditions. Proteins were transferred overnight to a PVDF membrane (Immobilion, Millipore, Bedford, MA). The membrane was then blocked with 5% blotting grade nonfat dry milk (Bio-Rad, Hercules, CA), and incubated with mouse monoclonal anti-MMP-1 antibody (Calbiochem, EMD, La Jolla, CA). HRP-conjugated anti-mouse IgG antibody (Santa Cruz Biotechnology, Santa Cruz, CA) was used as secondary antibody.

CXCL10 in FLS culture supernatants—5×10^6 FLS were grown on Matrigel-covered Petri dishes in 10 ml of complete media. Supernatants were collected and 500 μl were concentrated using Microcon YM-30 columns (Millipore) at 14,000 g for 10 minutes at room temperature. The same amount of protein concentrate per sample was loaded into a NuPAge Bis-Tris gel according to the protocol described above. A polyclonal rabbit IgG anti-rat CXCL10 antibody (Pierce, Thermo Scientific) was used as primary antibody, and an HRP-conjugated donkey anti-rabbit IgG antibody (Amersham-GE Healthcare) as secondary.

Intracellular calcium influx

Intracellular calcium influx was measured using the Fluo-4 NW calcium assay kit (Molecular Probes/Invitrogen) according to the manufacturer's instructions. Briefly, FLS were plated at a density of 4,500 cells/well in a 96-well plate (100 μl volume of complete media per well) and allowed to adhere. Media was then changed to serum-free and cells cultured overnight. Next morning the serum-free media was replaced with 50 μl of dye loading solution, and cells were incubated at 37°C for 30 minutes. AMG487 (100 μM for RA FLS and 10μM for DA FLS) or DMSO were then added to their respective wells and cultured at room temperature for 30 minutes, followed by a baseline fluorimetric reading. A solution with or without FBS was then added to bring the final concentration of FBS to 10%. Fluorescence was immediately measured with a Fluoroskan Ascent Microplate Fluorometer (Thermo Scientific) with settings appropriate for excitation at 494 nm and emission at 516 nm.

Immunofluorescence and confocal microscopy

Immunofluorescence was performed as previously reported (34, 35). Briefly, FLS were cultured on coverslips to 10–20% confluence, then starved overnight and treated with either DMSO or AMG487 in complete media. FLS were then fixed with 4% formaldehyde (Ted Pella INC, Redding, CA) for 15 minutes at room temperature followed by permeabilization with PBS/Triton X-100 0.1% for 5 minutes. Non-specific binding was blocked with 5% nonfat milk for 30 minutes. Cells were incubated with a rabbit antibody against phosphorylated FAK (Cell Signaling) for 1 hour at room temperature, washed and then incubated with Alexa Fluor 488 (green) donkey anti-rabbit IgG antibody (Invitrogen). Cells were washed with PBS and incubated with Alexa Fluor 594 (red) Phalloidin (actin filament staining; Invitrogen) for 15 minutes. The stained cells were washed with PBS, and mounted on a glass slide. A Zeiss Axiovert 200M fluorescent microscope was used for visualization with the appropriate filters, with Zeiss Axioversion 4.7 software. Immunofluorescence microscopy was used for cell cytoskeleton scoring (see below). Olympus FluoView 300 was used for confocal microscopy with a 600X magnification.

Actin cytoskeleton, lamellipodia and phospho-FAK scoring system

In order to quantify the potential changes induced by CXCR3 blockade in FLS morphology, we developed a new scoring system, which includes an established actin scoring system (36), plus the addition of scores for four major parameters of interest: a) actin filament characteristics and distribution (0 = no filaments, 1 = fine filament at the center of the cell, 2 = at least two thick filaments at the center of the cell, 3 = 90% thick filaments); b) cell morphology (0 = round shape, 2 = fusiforme/linearized shape); c) lamellipodia location (0 = no lamellipodia or presence all around the cell, 2 = polarized formation of lamellipodia on one side of the cell); d) distribution of phosphorylated FAK (0=on cell edges, 1 = homogeneous distribution, 2 = pronounced co-localization with lamellipodia). The cell scoring ranged from 0–9, and ten cells per treatment group and per cell line were analyzed.

MTT assay

4×10^4 FLS per well were plated in triplicate in 96-well plates in 100 μl of complete media. Cells were allowed to adhere for 24 hours. Media was then changed and either AMG487 or DMSO added at the specified concentrations. After 24 hours (same duration as the invasion experiments) viable cells were determined using the colorimetric MTT kit (Millipore) according to the manufacturer instructions.

Statistics

Means were analyzed with the Student's t-test or one-way ANOVA with a pairwise multiple comparison procedure (Holm-Sidak method) using SigmaStat 3.0 (SPSS, Chicago, IL).

RESULTS

CXCL10 significantly increases invasion of DA.F344(Cia5d) FLS in a CXCR3-dependent manner

DA.F344(Cia5d) FLS (minimally invasive) produced lower amounts of CXCL10 compared with DA FLS (highly invasive) (Figure 1A). To determine whether the reduced levels of CXCL10 explained the decreased invasiveness of DA.F344(Cia5d) FLS, invasion through Matrigel was studied in the presence or absence of CXCL10 (1μg/ml) in the lower chambers. CXCL10 treatment significantly increased the mean number of invading cells by 2-fold compared with controls (PBS-treated) (n=6; $p\leq0.005$, One way ANOVA, figure 1B). With CXCL10 treatment the DA.F344(Cia5d) FLS invasion reached 73.6% of the DA invasion (figure 1B; $p\leq0.005$, One Way ANOVA). Therefore, CXCL10 explains almost two-thirds of the difference in invasion between DA and DA.F344(Cia5d) FLS.

To confirm the specificity of the interaction between CXCL10 and its receptor CXCR3 in the regulation of the CXCL10-mediated invasion, a specific anti-CXCR3 blocking monoclonal antibody was used (200 μg/ml). Blockade of CXCR3 prevented the CXCL10-induced increase in FLS invasion, while an IgG1 isotype control did not, confirming the CXCR3 specificity (n=6; $p\leq0.005$, One Way ANOVA, Figure 1B).

Blockade of the CXCR3 receptor reduces DA FLS invasion and decreases levels of active MMP-1

Treatment of highly invasive DA FLS with anti-CXCR3 blocking antibody significantly decreased the number of cells invading through Matrigel over a 24 hour period by 40%, compared with the non-treated controls (n=6; $p\leq0.001$, t-test. Figure 1B).

To determine the effector mechanism of the CXCL10-CXCR3-mediated FLS invasion we analyzed protein levels of pro- and active MMP-1, MMP-2 and MMP-3 in supernatants of

DA FLS treated with or without anti-CXCR3 blocking antibody. Levels of active MMP-1 were significantly decreased and nearly undetectable in supernatants of DA FLS treated with anti-CXCR3 blocking antibody compared with the isotype controls (n=3; p=0.001, t-test. Figure 2A-B). No significant differences were detected for the other MMPs tested.

The CXCR3 small molecule inhibitor AMG487 significantly reduces cell invasion and the production of active MMP-1 by FLS from both DA rats and RA patients

The CXCR3 small molecule inhibitor AMG487 significantly reduced DA FLS invasion in a dose-dependent manner by as much as 77% at 10μM concentrations (n=8; p≤0.001, t-test. Figure 3A). AMG487 (100 μM) also significantly reduced invasion of FLS obtained from RA patients by 58% (n=6; p≤0.001, t-test. Figure 3B). We have determined that RA FLS express a higher level (two-fold) of CXCR3, compared with DA FLS, which is likely the reason for the requirement of higher concentrations of AMG487 to inhibit RA FLS invasion.

Similar to the results for anti-CXCR3 antibody neutralization experiments, AMG487-mediated blockade of CXCR3 also significantly reduced levels of active MMP-1 produced by DA FLS (Figure 4A and B, n=4; p=0.02, t-test).

CXCR3 blockade decreases intracellular calcium influx

The engagement of CXCR3 by CXCL10, which is present in FBS, activates the receptor and increases intracellular calcium influx in DA and RA FLS, compared with serum-free medium (figure 4C and D for DA and RA, respectively). Pre-treatment of FLS with the CXCR3 small molecule antagonist AMG487 reduced calcium influx in DA FLS by 64%, and by 100% (complete block) in RA FLS, confirming that the compound is interfering with CXCR3-mediated cell activation.

CXCR3 blockade interferes with actin cytoskeleton reorganization and lamellipodia formation

DA (figure 5A–C) and RA FLS (figure 5G–I) treated with DMSO (control) had very similar characteristics. Specifically, both DA and RA FLS had an elongated/fusiform morphology with increased numbers of thick and longitudinal actin filaments running parallel to each other and predominantly oriented in the same direction. The polarized shape consisted of a single broad leading edge at one side of the cells and a narrow trailing edge in the opposite direction. Lamellipodia were visible at the leading edge of the cells, and co-localized with phospho-FAK both in FLS from DA rats and from RA patients.

In contrast, AMG487-treated DA (figure 5D–F) and RA FLS (figure 5J–L) had a round and more compact morphology with a reduced number of actin stress fibers, which were often disorganized. AMG487-treated FLS didn't show a polarized orientation, resulting in aberrant leading edge formation. Lamellipodia like structures were occasionally seen in AMG487-treated cells, however those were present all around the cells as multiple narrow projections, and did not co-localize with the lamellipodia marker phospho-FAK.

We developed a scoring system to be able to quantify the above differences (see Methods). Both RA FLS and DA FLS treated with AMG487 had significantly reduced numbers of thick actin filaments, reduced numbers of elongated cells, reduced formation of polarized lamellipodia and reduced co-localization of phospho-FAK with lamellipodia, compared with DMSO-treated FLS (table 1).

DISCUSSION

The hyperplastic synovial tissue (pannus) in RA invades and destroys cartilage and bone, and the FLS has a central role in these processes (4–6). While joint destruction correlates with disease severity and with increased risk for disability, little is known about the genes regulating these processes. Previous studies have shown that the *in vitro* invasive properties of FLS through collagen-rich Matrigel correlate with histologic damage in rat PIA (7), and with radiographic erosions and damage in patients with RA (8). Therefore, we consider this model a useful strategy to understand the processes and genes regulating FLS invasion, and to identify new potential targets for therapies aimed at preserving joint architecture and reducing articular damage. Our previous studies with this model led to the identification of a FLS invasion-associated gene expression signature that included several genes implicated in cancer-related phenotypes, such as invasion and metastasis (13). CXCL10 was one of the most significantly up-regulated genes (4.6-fold) in highly invasive DA FLS (13).

In the present study we report increased production of CXCL10 protein by DA FLS, and show that treating minimally invasive DA.F344(Cia5d) FLS with CXCL10 significantly increased cell invasion in a CXCR3-dependent manner. Additionally, CXCL10 accounted for most of the difference in invasion between DA and DA.F344(Cia5d) FLS. CXCR3 blockade with either an antibody or a small molecule antagonist significantly reduced invasion of both DA FLS and RA FLS by as much as 86% and 53%, respectively. Our results demonstrate that blocking the CXCL10-CXCR3 engagement reduces CXCR3-mediated cell signaling as evidenced by the reduced intracellular calcium influx in FLS pre-treated with the small molecule CXCR3 antagonist AMG487. RA FLS calcium influx inhibition was more pronounced (100%) than the invasion suppressive effect (53%) most likely because these parameters involve different variables and different time-points. Specifically, calcium influx is a very early event during CXCR3 activation and in this case was used to measure the specific inhibition of CXCR3 signaling. On the other hand, while our studies show that CXCL10 has a major role in FLS invasion, it is clearly not the only mediator of invasion, thus its inhibition is not enough to completely block RA FLS invasion.

Additionally, blocking the CXCL10-CXCR3 interaction interfered with actin cytoskeleton reorganization and inhibited the polarized formation of lamellipodia, which is required for both cell migration and invasion. CXCR3 blockade also inhibited the formation of the active form of MMP-1, a collagenase implicated in cartilage and bone erosive changes.

Increased levels of CXCL10 have been previously reported in synovial fluid, synovial tissues and FLS from RA patients (20, 21). However, at the time it was mostly considered a chemoattractant for T cells and mast cells (19, 21, 37). CXCR3 was later found to be expressed by FLS (24). Antibodies against CXCL10 reduced disease severity in adjuvant-induced arthritis in rats (38), and in patients with RA in a placebo-controlled trial (39). However, the mechanism for the disease amelioration was only partially understood, and focused on the T cell. The present study identifies a new role for the CXCR3-CXCL10 interaction in the regulation of FLS invasion, and provides a new mechanistic explanation for the benefit described in previous *in vivo* studies.

MMP-1 levels have been previously correlated with joint damage in RA (40) and with the invasive properties of RA FLS (41, 42). However, this is the first time that FLS invasion and MMP-1 levels are shown to be regulated by CXCL10 and its receptor CXCR3. While MMP-1 can be activated by several serine proteases (43), it remains unclear whether CXCL10 activation of CXCR3 directly regulates MMP-1 activation, or whether it requires yet another molecule or pathway such as IL-1β.

There is strong evidence that CXCL10 increases the invasive and metastatic properties of cancer cells (14, 16, 17). While RA FLS and the RA synovial pannus invade local tissues in a tumor-like manner, they do not metastasize in the strict sense of the word. However, recent studies suggest that the FLS is able to migrate from the synovial tissue of an arthritic joint through the bloodstream, and home into a different and unaffected joint, where it is capable of spreading arthritis (44). Once at the new joint, the FLS then invades and destroys cartilage and bone (44). In order for the FLS to gain access to the blood stream, and then back into the synovial tissues of another joint, it likely requires chemotactic and invading signals such as those provided by CXCL10. Therefore, our discovery of a new role for CXCL10-CXCR3 in FLS invasion creates an additional parallel between RA FLS and cancer cell migration and invasion, and raises the possibility that blocking this pathway could not only reduce articular damage, but also reduce disease spreading from one joint to the other.

We were able to establish a previously unrecognized role for CXCL10 in the regulation of the invasive properties of FLS from arthritic DA rats and more importantly, FLS from patients with RA. We identified a new mechanistic explanation for the *in vivo* arthritis-improving effects of drugs or antagonistic antibodies reported by others (38, 39).

In conclusion, this study provides new evidence implicating CXCL10 and its receptor CXCR3 on the regulation of the *in vitro* invasive properties of FLS from patients with RA and rats with PIA. Since the *in vitro* invasive properties of FLS correlate with *in vivo* articular damage, our observations suggest that targeting CXCL10 and/or CXCR3 could be a the potentially useful strategy aimed at reducing articular damage and erosive changes in RA.

Acknowledgments

Funded by National Institutes of Health grants R01-AR46213, R01-AR052439 (NIAMS) and R01-AI54348 (NIAID) to Dr. P. Gulko.

The authors wish to thank Mary Keogh RN and Cathleen Mason RN of the Feinstein Institute’s Tissue Donation Program for their assistance in obtaining RA synovial tissues.

References

1. van Zeben D, Breedveld FC. Prognostic factors in rheumatoid arthritis. J Rheumatol Suppl. 1996; 44:31–3. [PubMed: 8833048]
2. Gossec L, Dougados M, Goupille P, Cantagrel A, Sibilia J, Meyer O, et al. Prognostic factors for remission in early rheumatoid arthritis: a multiparameter prospective study. Ann Rheum Dis. 2004; 63(6):675–80. [PubMed: 15140774]
3. Wolfe F, Mitchell DM, Sibley JT, Fries JF, Bloch DA, Williams CA, et al. The mortality of rheumatoid arthritis. Arthritis Rheum. 1994; 37(4):481–94. [PubMed: 8147925]
4. Muller-Ladner U, Kriegsmann J, Franklin BN, Matsumoto S, Geiler T, Gay RE, et al. Synovial fibroblasts of patients with rheumatoid arthritis attach to and invade normal human cartilage when engrafted into SCID mice. Am J Pathol. 1996; 149(5):1607–15. [PubMed: 8909250]
5. Gulko, PS.; Winchester, RJ. Rheumatoid arthritis. In: Austen, KF.; Frank, MM.; Atkinson, JP.; Cantor, H., editors. Samter’s Immunologic Diseases. 6. Baltimore: Lippincott, Williams & Wilkins; 2001. p. 427-63.
6. Bartok B, Firestein GS. Fibroblast-like synoviocytes: key effector cells in rheumatoid arthritis. Immunol Rev. 2010; 233(1):233–55. [PubMed: 20193003]
7. Laragione T, Brenner M, Mello A, Symons M, Gulko PS. The arthritis severity locus Cia5d is a novel genetic regulator of the invasive properties of synovial. Arthritis Rheum. 2008; 58(8):2296–306. [PubMed: 18668563]

8. Tolboom TC, van der Helm-Van Mil AH, Nelissen RG, Breedveld FC, Toes RE, Huizinga TW. Invasiveness of fibroblast-like synoviocytes is an individual patient characteristic associated with the rate of joint destruction in patients with rheumatoid arthritis. Arthritis Rheum. 2005; 52(7): 1999–2002. [PubMed: 15986342]

9. van Zeben D, Hazes JM, Zwinderman AH, Vandenbroucke JP, Breedveld FC. Factors predicting outcome of rheumatoid arthritis: results of a followup study. J Rheumatol. 1993; 20(8):1288–96. [PubMed: 8230007]

10. Welsing PM, van Gestel AM, Swinkels HL, Kiemeney LA, van Riel PL. The relationship between disease activity, joint destruction, and functional capacity over the course of rheumatoid arthritis. Arthritis Rheum. 2001; 44(9):2009–17. [PubMed: 11592361]

11. Drossaers-Bakker KW, de Buck M, van Zeben D, Zwinderman AH, Breedveld FC, Hazes JM. Long-term course and outcome of functional capacity in rheumatoid arthritis: the effect of disease activity and radiologic damage over time. Arthritis Rheum. 1999; 42(9):1854–60. [PubMed: 10513799]

12. Combe B, Dougados M, Goupille P, Cantagrel A, Eliaou JF, Sibilia J, et al. Prognostic factors for radiographic damage in early rheumatoid arthritis: a multiparameter prospective study. Arthritis Rheum. 2001; 44(8):1736–43. [PubMed: 11508423]

13. Laragione T, Brenner M, Li W, Gulko PS. Cia5d regulates a new fibroblast-like synoviocyte invasion-associated gene expression signature. Arthritis Res Ther. 2008; 10(4):R92. [PubMed: 18706093]

14. Zipin-Roitman A, Meshel T, Sagi-Assif O, Shalmon B, Avivi C, Pfeffer RM, et al. CXCL10 promotes invasion-related properties in human colorectal carcinoma cells. Cancer Res. 2007; 67(7):3396–405. [PubMed: 17409450]

15. Goldberg-Bittman L, Neumark E, Sagi-Assif O, Azenshtein E, Meshel T, Witz IP, et al. The expression of the chemokine receptor CXCR3 and its ligand, CXCL10, in human breast adenocarcinoma cell lines. Immunol Lett. 2004; 92(1–2):171–8. [PubMed: 15081542]

16. Kawada K, Sonoshita M, Sakashita H, Takabayashi A, Yamaoka Y, Manabe T, et al. Pivotal role of CXCR3 in melanoma cell metastasis to lymph nodes. Cancer Res. 2004; 64(11):4010–7. [PubMed: 15173015]

17. Walser TC, Rifat S, Ma X, Kundu N, Ward C, Goloubeva O, et al. Antagonism of CXCR3 inhibits lung metastasis in a murine model of metastatic breast cancer. Cancer Res. 2006; 66(15):7701–7. [PubMed: 16885372]

18. Ma X, Norsworthy K, Kundu N, Rodgers WH, Gimotty PA, Goloubeva O, et al. CXCR3 expression is associated with poor survival in breast cancer and promotes metastasis in a murine model. Mol Cancer Ther. 2009; 8(3):490–8. [PubMed: 19276169]

19. Hanaoka R, Kasama T, Muramatsu M, Yajima N, Shiozawa F, Miwa Y, et al. A novel mechanism for the regulation of IFN-gamma inducible protein-10 expression in rheumatoid arthritis. Arthritis Res Ther. 2003; 5(2):R74–81. [PubMed: 12718750]

20. Ueno A, Yamamura M, Iwahashi M, Okamoto A, Aita T, Ogawa N, et al. The production of CXCR3-agonistic chemokines by synovial fibroblasts from patients with rheumatoid arthritis. Rheumatol Int. 2005; 25(5):361–7. [PubMed: 15004722]

21. Patel DD, Zachariah JP, Whichard LP. CXCR3 and CCR5 ligands in rheumatoid arthritis synovium. Clin Immunol. 2001; 98(1):39–45. [PubMed: 11141325]

22. Kuan WP, Tam LS, Wong CK, Ko FW, Li T, Zhu T, et al. CXCL 9 and CXCL 10 as Sensitive markers of disease activity in patients with rheumatoid arthritis. J Rheumatol. 2010; 37(2):257–64. [PubMed: 20032101]

23. Lacotte S, Brun S, Muller S, Dumortier H. CXCR3, inflammation, and autoimmune diseases. Ann N Y Acad Sci. 2009; 1173:310–7. [PubMed: 19758167]

24. Garcia-Vicuna R, Gomez-Gaviro MV, Dominguez-Luis MJ, Pec MK, Gonzalez-Alvaro I, Alvaro-Gracia JM, et al. CC and CXC chemokine receptors mediate migration, proliferation, and matrix metalloproteinase production by fibroblast-like synoviocytes from rheumatoid arthritis patients. Arthritis Rheum. 2004; 50(12):3866–77. [PubMed: 15593223]

25. Brenner M, Meng HC, Yarlett NC, Joe B, Griffiths MM, Remmers EF, et al. The Non-MHC Quantitative Trait Locus Cia5 Contains Three Major Arthritis Genes That Differentially Regulate

Disease Severity, Pannus Formation, and Joint Damage in Collagen- and Pristane-Induced Arthritis. J Immunol. 2005; 174(12):7894–903. [PubMed: 15944295]

26. Joe B, Remmers EF, Dobbins DE, Salstrom JL, Furuya T, Dracheva S, et al. Genetic dissection of collagen-induced arthritis in Chromosome 10 quantitative trait locus speed congenic rats: evidence for more than one regulatory locus and sex influences. Immunogenetics. 2000; 51(11):930–44. [PubMed: 11003387]
27. Vingsbo C, Sahlstrand P, Brun J, Jonsson R, Saxne T, Holmdahl R. Pristane-induced arthritis in rats: A new model for rheumatoid arthritis with a chronic disease course influenced by both major histocompatibility complex and non-major histocompatibility complex genes. Am J Pathol. 1996; 149:1675–83. [PubMed: 8909256]
28. Brenner M, Meng H, Yarlett N, Griffiths M, Remmers E, Wilder R, et al. The non-MHC quantitative trait locus Cia10 contains a major arthritis gene and regulates disease severity, pannus formation and joint damage. Arthritis Rheum. 2005; 52(1):322–32. [PubMed: 15641042]
29. Arnett FC, Edworthy SM, Bloch DA, McShane DJ, Fries JF, Cooper NS, et al. The American Rheumatism Association 1987 revised criteria for the classification of rheumatoid arthritis. Arthritis Rheum. 1988; 31(3):315–24. [PubMed: 3358796]
30. Johnson M, Li AR, Liu J, Fu Z, Zhu L, Miao S, et al. Discovery and optimization of a series of quinazolinone-derived antagonists of CXCR3. Bioorg Med Chem Lett. 2007; 17(12):3339–43. [PubMed: 17448658]
31. Michael IP, Sotiropoulou G, Pampalakis G, Magklara A, Ghosh M, Wasney G, et al. Biochemical and enzymatic characterization of human kallikrein 5 (hK5), a novel serine protease potentially involved in cancer progression. J Biol Chem. 2005; 280(15):14628–35. [PubMed: 15713679]
32. Ghosh MC, Grass L, Soosaipillai A, Sotiropoulou G, Diamandis EP. Human kallikrein 6 degrades extracellular matrix proteins and may enhance the metastatic potential of tumour cells. Tumour Biol. 2004; 25(4):193–9. [PubMed: 15557757]
33. Sasaki M, Kashima M, Ito T, Watanabe A, Izumiyama N, Sano M, et al. Differential regulation of metalloproteinase production, proliferation and chemotaxis of human lung fibroblasts by PDGF, interleukin-1beta and TNF-alpha. Mediators Inflamm. 2000; 9(3–4):155–60. [PubMed: 11132772]
34. Chan A, Akhtar M, Brenner M, Zheng Y, Gulko PS, Symons M. The GTPase Rac Regulates the Proliferation and Invasion of Fibroblast-Like Synoviocytes from Rheumatoid Arthritis Patients. Mol Med. 2007; 13(5–6):297–304. [PubMed: 17622308]
35. Laragione T, Gulko PS. mTOR regulates the invasive properties of synovial fibroblasts in rheumatoid arthritis. Mol Med. 2010; 16(9–10):352–8. [PubMed: 20517583]
36. Verderame M, Alcorta D, Egnor M, Smith K, Pollack R. Cytoskeletal F-actin patterns quantitated with fluorescein isothiocyanate-phalloidin in normal and transformed cells. Proc Natl Acad Sci U S A. 1980; 77(11):6624–8. [PubMed: 6256751]
37. Ruschpler P, Lorenz P, Eichler W, Koczan D, Hanel C, Scholz R, et al. High CXCR3 expression in synovial mast cells associated with CXCL9 and CXCL10 expression in inflammatory synovial tissues of patients with rheumatoid arthritis. Arthritis Res Ther. 2003; 5(5):R241–52. [PubMed: 12932287]
38. Salomon I, Netzer N, Wildbaum G, Schif-Zuck S, Maor G, Karin N. Targeting the function of IFN-gamma-inducible protein 10 suppresses ongoing adjuvant arthritis. J Immunol. 2002; 169(5): 2685–93. [PubMed: 12193742]
39. Yellin M, Paliienko I, Balanescu A, Vizir V, Ter-Vartanian S, Tian J, et al. A Phase II, Randomized, Double-Blind, Placebo-Controlled Study To Evaluate The Efficacy And Safety Of MDX-1100, A Fully Human Anti-CXCL10 Monoclonal Antibody, In Combination With Methotrexate (MTX) In Patients With Rheumatoid Arthritis (RA). Arthritis Rheum. 2009; 60 (suppl 10):414.
40. Cunnane G, Fitzgerald O, Beeton C, Cawston TE, Bresnihan B. Early joint erosions and serum levels of matrix metalloproteinase 1, matrix metalloproteinase 3, and tissue inhibitor of metalloproteinases 1 in rheumatoid arthritis. Arthritis Rheum. 2001; 44(10):2263–74. [PubMed: 11665967]
41. Tolboom TC, Pieterman E, van der Laan WH, Toes RE, Huidekoper AL, Nelissen RG, et al. Invasive properties of fibroblast-like synoviocytes: correlation with growth characteristics and

expression of MMP-1, MMP-3, and MMP-10. Ann Rheum Dis. 2002; 61(11):975–80. [PubMed: 12379519]

42. Rutkauskaite E, Zacharias W, Schedel J, Muller-Ladner U, Mawrin C, Seemayer CA, et al. Ribozymes that inhibit the production of matrix metalloproteinase 1 reduce the invasiveness of rheumatoid arthritis synovial fibroblasts. Arthritis Rheum. 2004; 50(5):1448–56. [PubMed: 15146414]
43. Saunders WB, Bayless KJ, Davis GE. MMP-1 activation by serine proteases and MMP-10 induces human capillary tubular network collapse and regression in 3D collagen matrices. J Cell Sci. 2005; 118(Pt 10):2325–40. [PubMed: 15870107]
44. Lefevre S, Knedla A, Tennie C, Kampmann A, Wunrau C, Dinser R, et al. Synovial fibroblasts spread rheumatoid arthritis to unaffected joints. Nat Med. 2009

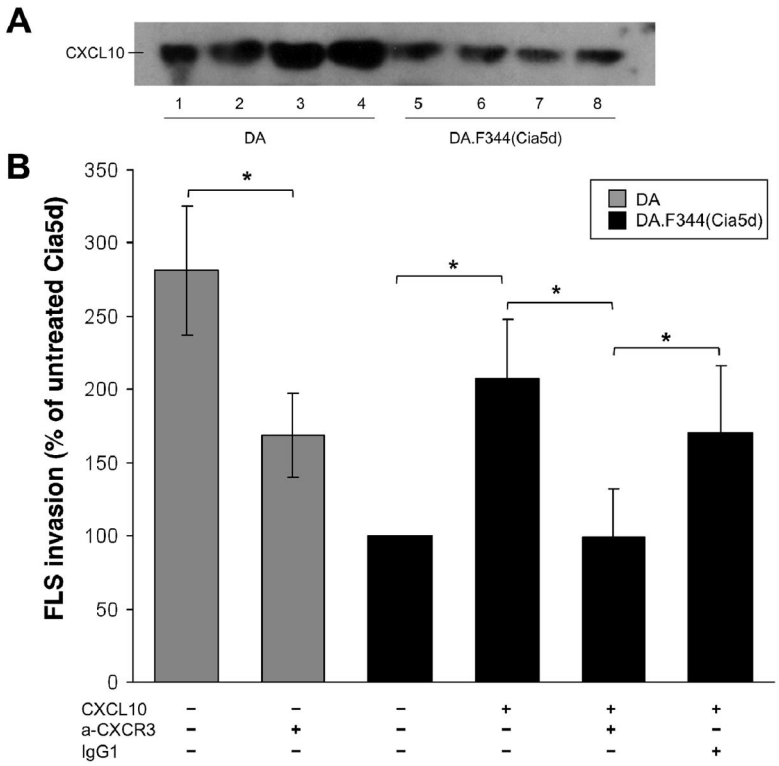

FIGURE 1. CXCL10 regulates FLS invasion in a CXCR3-dependent manner and explains most of the difference in invasion between DA and DA.F344(Cia5d)

(A) Highly invasive DA FLS produce increased levels of CXCL10 compared with minimally invasive DA.F344(Cia5d) FLS (western blot done with supernatants of FLS cultured on Matrigel; see methods for details). **(B)** DA FLS treated with anti-CXCR3 were significantly less invasive (40% reduction), compared with untreated DA controls (n=6; *P≤0.001; One way ANOVA). DA.F344(Cia5d) FLS treated with CXCL10 (1μg/ml) increased invasion by 2-fold, compared with untreated controls, and became 73% as invasive as DA. Anti-CXCR3 antibodies (200μg/ml), but not an IgG1 isotype control (200μg/ml), prevented the CXCL10-induced increase in FLS invasion (Matrigel invasion assay; n=6; *P≤0.001, One way ANOVA; mean±S.D.). Percentage changes are all compared with untreated DA.F344(Cia5d).

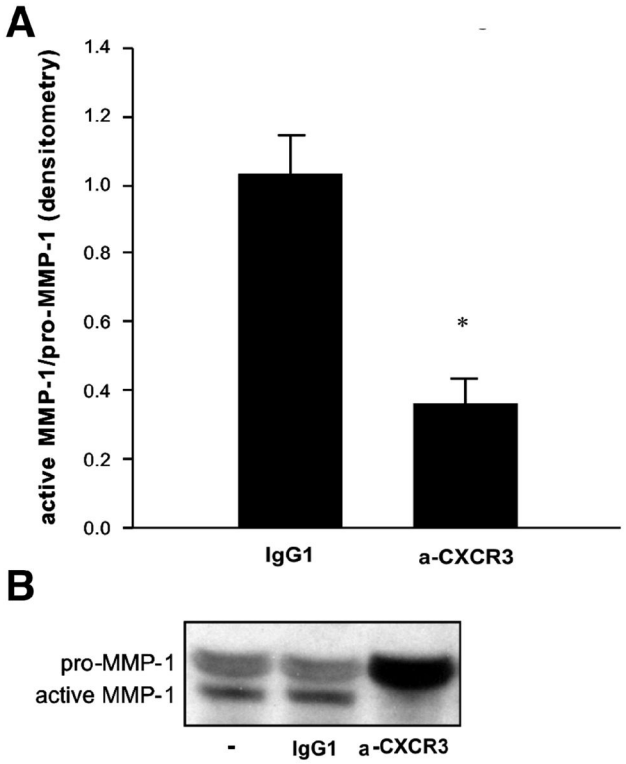

FIGURE 2. Anti-CXCR3 antibodies significantly reduce DA FLS production of activated MMP-1

(A) Densitometry analyses showing that anti-CXCR3 treatment significantly reduced DA FLS production of active MMP-1 (n=3; *P=0.001; t-test; mean±S.D.). **(B)** Representative western blot of the above densitometries demonstrating significant reduction in the levels of active form of MMP-1 in supernatants of FLS treated with anti-CXCR3, compared with no-treatment and isotype control.

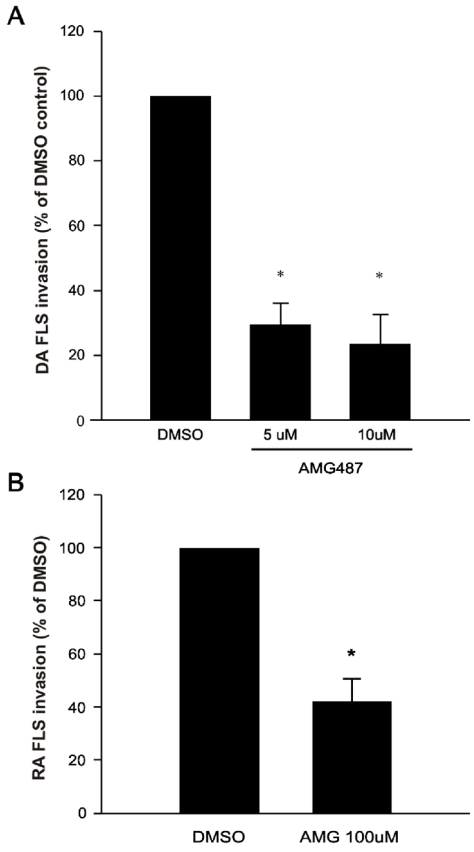

FIGURE 3. The CXCR3 small antagonist AMG487 decreases invasion of both DA and RA FLS

(A) DA (n=8; *P≤0.001, t-test) and **(B)** RA (n=6; *P≤0.001, t-test; mean±S.D.) FLS invasion was significantly reduced by 77% and 58%, respectively, with AMG487 10μM treatment, compared with control.

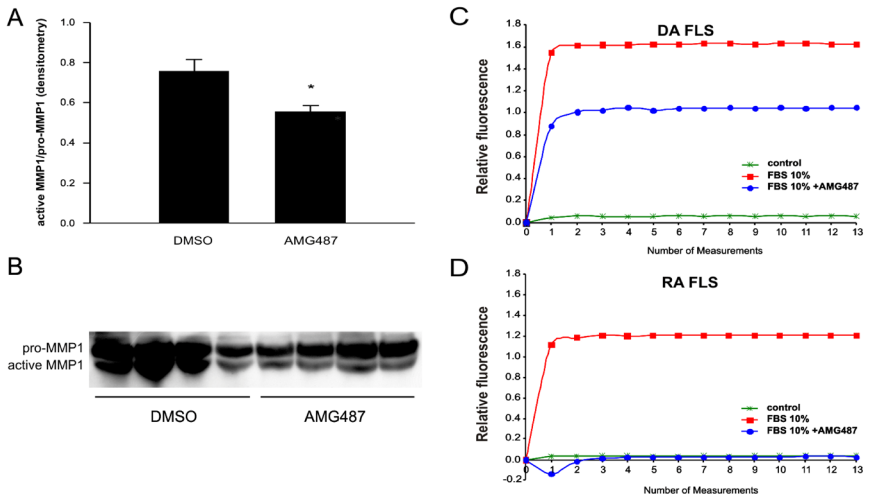

FIGURE 4. AMG487 reduces production of active MMP-1 and CXCR3-mediated calcium influx into DA and RA FLS

(A) Densitometry analyses of MMP-1 western blot (below) of four DA FLS cell lines (mean of active/pro-MMP-1). (*P=0.02, t-test; mean±S.E.M.). **(B)** Western blot showing pro- and active MMP-1 (n=4). **(C)** CXCL10-containing 10% FBS induced a significant increase in intracellular calcium influx. Pre-treatment of FLS with AMG487 (10μM) reduced calcium influx by nearly 64% in DA FLS, **(D)** and by 100% in RA FLS (AMG487 100 μM), compared with FLS treated with 10% FBS only, confirming inhibition of the CXCR3 receptor signaling.

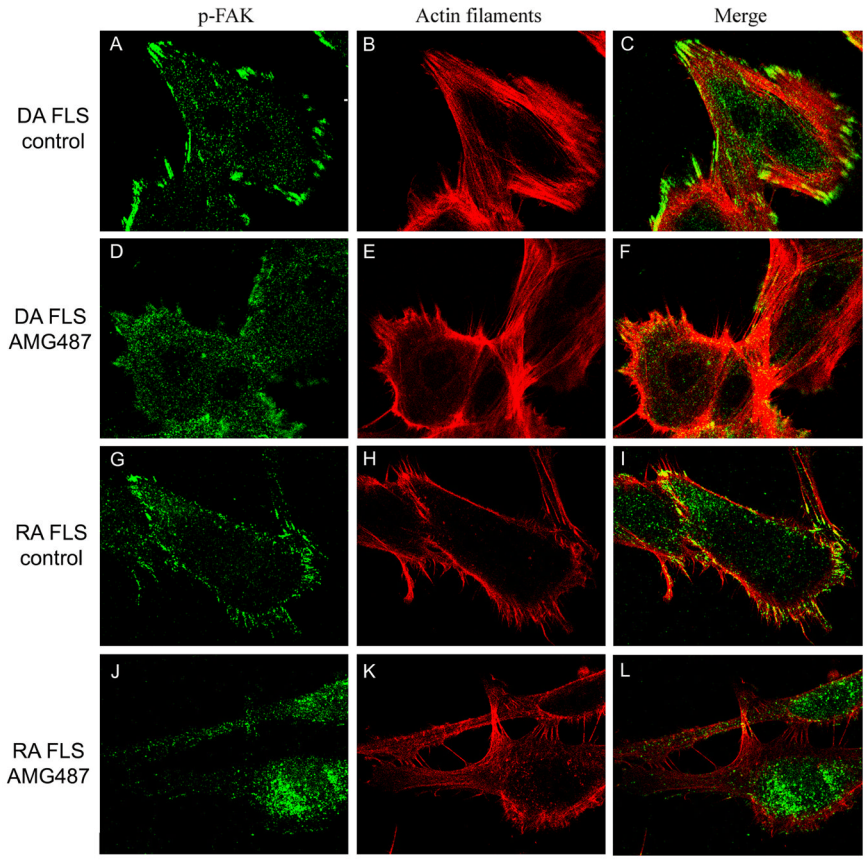

FIGURE 5. CXCR3 blockade with AMG487 inhibits actin filament reorganization and prevents the polarized formation of lamellipodia

(A–C) DA FLS treated with DMSO (control) had linearized actin filaments (Alexa Fluor 594-phalloidin: red), elongated shape and lamellipodia at the leading edge of the cells. **(D–F)** DA FLS treated with AMG487 10μM had a round shape, fewer actin filaments and reduced number of lamellipodia, which did not co-localize with phospho-FAK (Alexa Fluor 488: green). **(G–I)** RA FLS treated with DMSO and those treated with AMG487 100μM **(J–L)** had similar characteristics to DA FLS receiving the same treatments.

Table 1

FLS morphology scoring in cell treated with DMSO or the CXCR3 antagonist AMG487*

	DA (n=3)		RA (n=4)	
	control	**AMG487**	**control**	**AMG487**
Actin				
no filaments	0	6.7	0	7.5
fine filaments at the center	0	43.3	30	77.5
>2 thick fillaments at the center	0	40	20	10
90% thick filament	100	10	50	5
Cell shape				
Round	0	50	2.5	12.5
Elongated	100	50	97.5	87.5
Lamellipodia				
none or all around cell	0	90	2.5	97.5
polarized (on one side)	100	10	97.5	2.5
p-FAK				
cell edges	0	43.3	0	40
homogenous distribution	0	46.7	7.5	60
co-localization with lamellipodia	100	10	92.5	0

* Percentage of cells within each treatment group that met the specified category criteria.

The most significant differences are shown in light grey.

Ten cells per treatment group and per cell line were analyzed.

DA and RA FLS were treated with AMG487 10μM and 100μM, respectively.